doi:10.3969/j.issn.1673-4785.2011.01.012

Fuzzy logic for large mining bucket wheel reclaimer motion control—from an engineer's perspective

LU Tienfu

(School of Mechanical Engineering, University of Adelaide, North Terrace Adelaide, South Australia SA 5005, Australia)

Abstract: The bucket wheel reclaimer (BWR) is a key piece of equipment which has been widely used for stacking and reclaiming bulk materials (i.e. iron ore and coal) in places such as ports, iron-steel plants, coal storage areas, and power stations from stockpiles. BWRs are very large in size, heavy in weight, expensive in price, and slow in motion. There are many challenges in attempting to automatically control their motion to accurately follow the required trajectories involving uncertain parameters from factors such as friction, turbulent wind, its own dynamics, and encoder limitations. As BWRs are always heavily engaged in production and cannot be spared very long for motion control studies and associated developments, a BWR model and simulation environment closely resembling real life conditions would be beneficial. The following research focused mainly on the implementation of fuzzy logic to a BWR motion control from an engineer's perspective. First, the modeling of a BWR including partially known parameters such as friction force and turbulence to the system was presented. This was then followed by the design of a fuzzy logic-based control built on a model-based control loop. The investigation provides engineers with an example of applying fuzzy logic in a model based approach to properly control the motion of a large BWR following defined trajectories, as well as to show possible ways of further improving the controller performance. The result indicates that fuzzy logic can be applied easily by engineers to overcome most motion control issues involving a large BWR.

Keywords: bucket wheel reclaimer; modeling; simulation; motion control; fuzzy logic

CLC Number: TP273.4　**Document code**: A　**Article ID**: 1673-4785(2011)01-0085-10

The Australian mineral industry has played an important role in Australia's economy for years. A snapshot shows that it represented 26% of Australian capital investment, 8% of total national GDP, and 40% of total trade in the 2006—2007 fiscal year. The industry is mostly located in rural and remote Australia, and contributes vast sums to the taxation and royalty revenues of the Australian Governments.

The mining industry is one of the most important export industries in Australia. Mining covers a broad spectrum of activities, from exploring and identifying new ore bodies such as coal, to processing, transportation, and exporting. Before solid bulk materials such as metal ores are exported, they are normally stockpiled at ports while waiting to be reclaimed according to the desired quality and quantity combinations, and subsequently loaded to ships.

The presented work concerns the motion control issues which have arisen due to the uncertainties caused by the insufficient knowledge and modeling errors of the bucket wheel reclaimer (BWR) that are normally associated with stacking and reclaiming stockpiles[1] in port areas.

Anyone who knows the field would agree that there are a lot more areas regarding the operations associated with BWRs which could be further developed, including improving the efficiency of BWR motion control. Nevertheless, stockpiles and BWRs within a stockyard are always heavily engaged and stretched to production limits. As they often cannot be spared for the required time period of research and development in order to improve operation efficiencies, alternatives are required. One of the choices is simulation. By properly reflecting the physics in areas such as uncertainty in computer simulation environments, research and development can be carried out without interrupting the production operation of real BWRs until the very late stages involving fine tuning and implementations.

Received Date: 2010-09-25.

Corresponding Author: LU Tienfu. E-mail: tien-fu.lu@adelaide.edu.au.

From the perspective of controlling the motion of such large machinery (BWR in this case), one of the key challenges lies in the imperfect knowledge about the system. It is not difficult to derive correct kinematics (forward and inverse), but it is extremely difficult to obtain accurate dynamics which include all the effects acting on the large machine such as frictional and environmental forces (i. e. impact forces which interact with the environment and turbulent forces caused by wind). Rather than using the real BWR which is heavily engaged in production, this study first develops a simulation model to reflect the imperfect knowledge of the system, especially in relation to dynamics. Then based on such a model, a fuzzy logic based controller is developed to follow the designed motion trajectory.

To model a typical BWR, its kinematics and dynamics which describe the behaviours and motions of the BWR are essential. So far, very few studies have been published in the public domain for BWR modelling. In 1997, Choi et al[2]. solved the inverse kinematics of a BWR using a false position method. The extracted contour lines which resulted from a 3-dimentional range finder were viewed as reclaiming patches on which the ore can be extracted. The BWR was treated as 4 degrees of freedom robotic manipulator possessing redundancy in its kinematics. Furthermore, the inverse kinematics problem of a BWR was extensively investigated by Choi et al. in 1999[3] and Hong and Choi in 2000[4]. The inverse kinematics problem was solved for both whole stockpile reclaiming and layer reclaiming. The key focus of those studies was to find an optimal landing point for reclaiming to prevent overload which occurrs when the buckets dig ore deeper than the prescribed scooping depth. The proposed automatic landing algorithm successfully implemented for the reclaimer in Kwangyang Steelworks, Korea. Positional errors of 20 cm resulted between the trajectory of the buckets and the surface of the pile. Error boundaries were said to be acceptable because the bucket length and width were about 80 and 40 cm respectively. Nevertheless, there was no similar modelling work presented in the study to reflect a real BWR model for controller design and related research as demonstrated by the presented study.

In this paper, Section I presents the modelling of a typical BWR including its kinematics and dynamics, as well as the imperfect knowledge of the system (uncertainties), through the modelling of friction forces, encoder limitations, and unexpected disturbances as the part of the system which is unknown to the controller. Section Ⅱ presents fuzzy logic that will be used to deal with the modelling uncertainties and errors. In section Ⅲ controller design using fuzzy logic on top of a model-based portion is presented. Section Ⅳ presents trajectory generation, and Section Ⅴ gives simulation results and discussions. Finally, the conclusions are presented in Section Ⅵ.

1 Bucket wheel reclaimer modeling

Fig. 1 below shows the simplified mining operation process regarding the flow of iron ores. It depicts which two stages of bulk materials are stockpiled and subsequently reclaimed, in this case using BWRs.

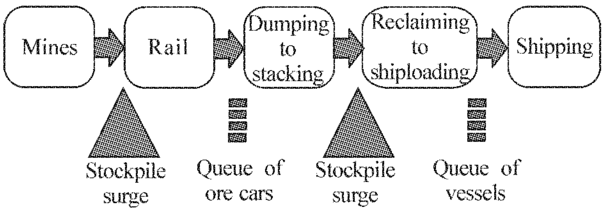

Fig. 1 Flow of bulk materials

BWRs have been widely adopted in mining industry for stacking and reclaiming stockpiles as shown in Fig. 2. To this point, BWRs are still mostly manually operated[5], remotely operated, or automated to follow simple predefined trajectory patterns with no flexibility of real-time automatic trajectory change when needed. With bulk handling facilities stretched to mechanical limits in order to meet market demands, the efficiency and motion accuracy gained through improved control will be of great benefit[6].

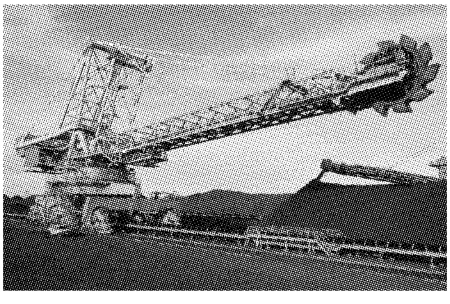

Fig. 2 KRUPP bucket wheel reclaimer

From a modeling perspective, a typical BWR can normally be treated as having 3 degrees of freedom excluding the rotating bucket wheel. The first degree of freedom (axis 1) comes from a linear track located at the bottom of the BWR, as shown in Fig. 3. This prismatic axis is represented by a rectangular box with a black dot in it. The linear track allows the BWR to move linearly and therefore is a prismatic joint using robotic terminology. The second degree of freedom (axis 2) comes from the luff motion which swings the boom. This axis is represented by a vertical line pointing up with an arrow. The third degree of freedom (axis 3) comes from the slew motion which rotates the boom up and down. This axis is represented by a circle with a black dot in it. Therefore, a typical BWR can be treated as a PRR (prismatic-revolute-revolute) robotic arm.

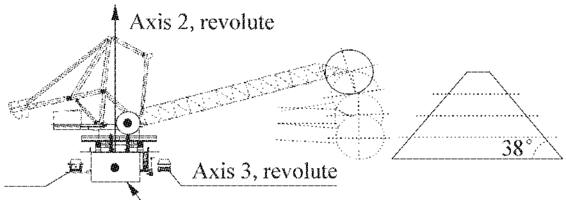

Fig. 3　A drawing of a bucket wheel reclaimer on the left and a stockpile on the right

As the kinematics and dynamics of a BWR have been derived and presented, in the following section, the final equations are extracted and listed. The details of the derivations can be found in the author's previous work[3,5].

Based on the assumption that the BWR studied here has the parameters listed in Table 1 and joint limits listed in Equ. (1), which are subject to changes since different BWRs will have different parameters, the following kinematics and dynamics were derived.

Table 1　Parameters of the BWR　m

L_2	L_3	L_4	L_5
6	5	5	50

$$\begin{cases} -25\ \text{m} \leqslant d_1 \leqslant 25\ \text{m}, \\ -90° < \theta_2 < 90°, \\ -15° < \theta_3 < 15°. \end{cases} \tag{1}$$

1) BWR kinematics.

The BWR's forward kinematics are shown in Equ. (2).

$${}^0_4T = \begin{bmatrix} \sin\theta_2\sin\theta_3 & \cos\theta_2 & -\sin\theta_2\cos\theta_3 & -\sin\theta_2(50\cos\theta_3+5) \\ -\cos\theta_3 & 0 & -\sin\theta_3 & -50\sin\theta_3-11 \\ -\cos\theta_2\sin\theta_3 & \sin\theta_2 & \cos\theta_2\cos\theta_3 & 50\cos\theta_2\cos\theta_3+5\cos\theta_2+d_1 \\ 0 & 0 & 0 & 1 \end{bmatrix}. \tag{2}$$

The BWR's inverse kinematics are shown in Equ. (3) below:

$$\begin{aligned} \theta_3 &= A\tan2[(-y-11),(\sqrt{50^2-(y+11)^2})], \\ \theta_2 &= A\sin\left(\frac{-x}{50\cos\theta_3+5}\right), \\ d_1 &= z-50\cos\theta_2\cos\theta_3-5\cos\theta_2. \end{aligned} \tag{3}$$

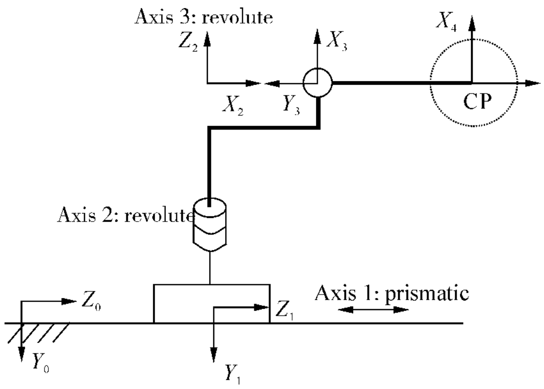

Fig. 4　BWR motion axes

With reference to Fig. 4, θ_i is the angle between X_{i-1} and X_i measured about Z_i. L_i is the distance from Z_i to Z_{i+1} measure along X_i. d_i is the distance from X_{i-1} to X_i measured along Z_i.

With the given desired (x, y, z) coordinate for the CP (centre point of the bucket wheel) to reach, the sequence of solving the inverse kinematics starts from θ_3 and finishes at obtaining d_1.

2) BWR dynamics.

As the real structure of the BWR is complicated as can be seen in Fig. 2 and not readily available for this study, the mass distributions of the linkages are thus simplified and assumed to be point masses which should be still appropriate for the construction of a reasonable model. The locations of the point masses are detailed in the author's previous investigation[6]. The general joint state space dynamic equation can be expressed as:

$$\boldsymbol{\tau} = \boldsymbol{M}(\theta)\ddot{\theta} + \boldsymbol{V}(\theta,\dot{\theta}) + \boldsymbol{G}(\theta).$$

Where $\boldsymbol{M}$ is a 3×3 mass matrix, $\boldsymbol{V}$ is a 3×1 vector for Corilois/Centrifugal forces and $\boldsymbol{G}$ is a 3×1 gravity vector. The equations for the mass matrix and vectors are listed below.

$$\boldsymbol{M}(\theta) = \begin{bmatrix} m(1,1) & 0 & m(1,3) \\ 0 & m(2,2) & m(2,3) \\ m(3,1) & m(3,2) & m(3,3) \end{bmatrix}.$$

Where,

$$m(1,1) = \frac{25m_2}{4} + 25m_3(1 + 10\cos\theta_3) + 625m_3\cos^2\theta_3,$$

$$m(1,3) = m(3,1) = -\frac{1}{2}\sin\theta_2(5m_2 + 10m_3 + 50m_3\cos\theta_3),$$

$$m(2,2) = 625m_3,$$

$$m(2,3) = m(3,2) = -25m_3\sin\theta_3\cos\theta_2,$$

$$m(3,3) = m_1 + m_2 + m_3,$$

$$\boldsymbol{V}(\theta,\dot{\theta}) = \begin{bmatrix} V(1,1) \\ V(2,1) \\ V(3,1) \end{bmatrix}.$$

Where,

$$V(1,1) = -25m_3\dot{\theta}_2\dot{\theta}_3\sin\theta_3(1 + 5\cos\theta_3),$$

$$V(2,1) = 125m_3\dot{\theta}_2^2\sin\theta_3(1 + 5\cos\theta_3),$$

$$V(3,1) = -2.5m_2\dot{\theta}_2^2\cos\theta_2 - 5m_3\dot{\theta}_2^2\cos\theta_2 - 25m_3\dot{\theta}_2^2\cos\theta_2\cos\theta_3 + 50m_3\dot{\theta}_2\dot{\theta}_3\sin\theta_2\sin\theta_3 - 25m_3\dot{\theta}_3^2\cos\theta_2\cos\theta_3,$$

$$\boldsymbol{G}(\theta) = \begin{bmatrix} 0 \\ 25m_3 g\cos\theta_3 \\ 0 \end{bmatrix}.$$

3) Modeling of friction forces.

The dynamic equations derived above do not cover all the forces acting on the BWR, including friction. In order to create a simulation environment that can reflect the imperfect knowledge of the system, it is important to model friction forces such as disturbances and errors coming from encoders as the parts of the system that are unknown to the controller. There are two friction forces to be modelled, viscous friction and Coulomb friction. Nevertheless, in this study, a vector of friction coefficients for three joints is set as the gain, [0.05, 0.05, 0.05] which is multiplied by the joint velocities to generate friction forces similar to viscous friction forces. These gains can later be changed for more accurate results or even replaced by the combination of Coulomb and viscous friction forces.

The more complete dynamic model becomes:

$$\boldsymbol{\tau} = \boldsymbol{M}(\theta)\ddot{\theta} + \boldsymbol{V}(\theta,\dot{\theta}) + \boldsymbol{G}(\theta) + \boldsymbol{F}(\theta,\dot{\theta}).$$

4) Modeling of encoders.

Encoders are normally attached to the joints to record their motions (i. e. how many degrees the joint has rotated). However, they are limited by their resolutions to interpret the motion of joints. As the encoder output is discrete, there will be errors caused by resolution limitation. In the presented study, quantiser blocks using Simulink are incorporated to simulate the discrete nature and errors resulting from the limited resolutions of encoders.

Assuming all the position encoders consisting of the 2nd and 3rd (luff and slew) joints have 4 096 bits per revolution, the long travel encoder is directly coupled to a non-drive bogie wheel axel with a wheel circumference about 2 m. Thus, the resolution is 360 (degrees)/4 096 = 0.087 89 degrees, which is equivalent to 0.001 533 4 radians. The quantization intervals for the three encoders are therefore set at 0.001 533 4 for the presented study.

5) Modeling of disturbances.

In order to model more realistically, a vector with a random disturbance force/torque was applied at all three joints, τ_d, which have the random values between 100 and −100 (kg for prismatic joint and kg-m for revolute joints) with a mean value of zero while acting to disturb the system is introduced into the control system. This external noise is introduced to partially cover the combined influences of modelling inaccuracies caused by factors such as simplifying the dynamics, un-modelled bucket wheels, and scooped materials in the bucket wheels.

2 Fuzzy logic

It is always difficult for an expert to represent the required knowledge to solve an engineering problem using vague and ambiguous computer terms until certain artificial techniques such as fuzzy logic are available. From an engineer's perspective, using engineering common sense in vague and ambiguous terms to solve engineering problems is intuitive and even preferred in many cases. For example, to prevent a motor from running too hot, it is much easier to describe the control actions required in vague and ambiguous terms, such as "if the motor is overheating, you must slow it down" than set conditions in crisp numbers.

Fuzzy logic is multi-valued logic. It allows any degree of value from 0 to 1 to be assigned in a fuzzy set, such as gray instead of black or white. This is different from crisp logic, where given items are either members of a definite set or they are not. It is therefore possible to have a reasoning system which makes decisions by combing set membership distributions. This gives great flexibility in making decisions based upon degrees of truth when facing uncertainties that are too difficult or cumbersome to be defined using crisp numbers. However, there must be a set of rules, where the conjunction "and" calls for the minimum membership of the topic being considered to yield an output membership value for decision-making purposes[7]. As a result, fuzzy logic has been widely adopted and applied for the entire span of engineering applications and products ranging from manufacturing machinery to domestic appliances (i. e. the washing machine).

Engineers normally are short of time in dealing with one given problem. They need to effectively solve the given problem and move on as soon as possible as there are always plenty problems waiting to be resolved. Many engineers would wish to have more time to conduct thorough studies and investigations for the best solutions before moving on, but such a wish is not normally granted.

When solving problems concerning uncertainties having values other than false and true (0 and 1), fuzzy logic could potentially be a good choice. When engineers try to apply fuzzy logic to solve the engineering problems, normally not enough attention is paid to the complicated mathematics behind the user interface to perform such fuzzification and defuzzification. Instead, focus is given to choosing one of the readily available software programs that most likely share a similar graphical user interface, similar ways of entering fuzzy logic rules, and similar methods of setting up membership sets based on his/her preferences. Of course, ultimately, the chosen software will still need to deliver satisfactory results.

Depending on the nature of the problems to be resolved using fuzzy logic, engineers will need to look into aspects of setting up the fuzzy logic parameters including numbers of input/output, fuzzy logic rules, range of membership sets, and input/output scaling. These factors will be detailed in the next section.

3 Controller design

The size of a BWR is large (i. e. 50 meter long boom which is the length of one link) and therefore it normally moves slowly. In the author's previous work, a model-based controller was developed. However, the performance of a model-based controller is indeed sensitive to modeling errors and unexpected disturbances in addition to the need of laboriously finding appropriate gains. Hence, fuzzy logic is adopted and implemented to deal with the modeling errors and uncertainties on top of the model based portion, which is limited by the lack of knowledge about the system, to improve the BWR's motion performances as shown in Fig. 5.

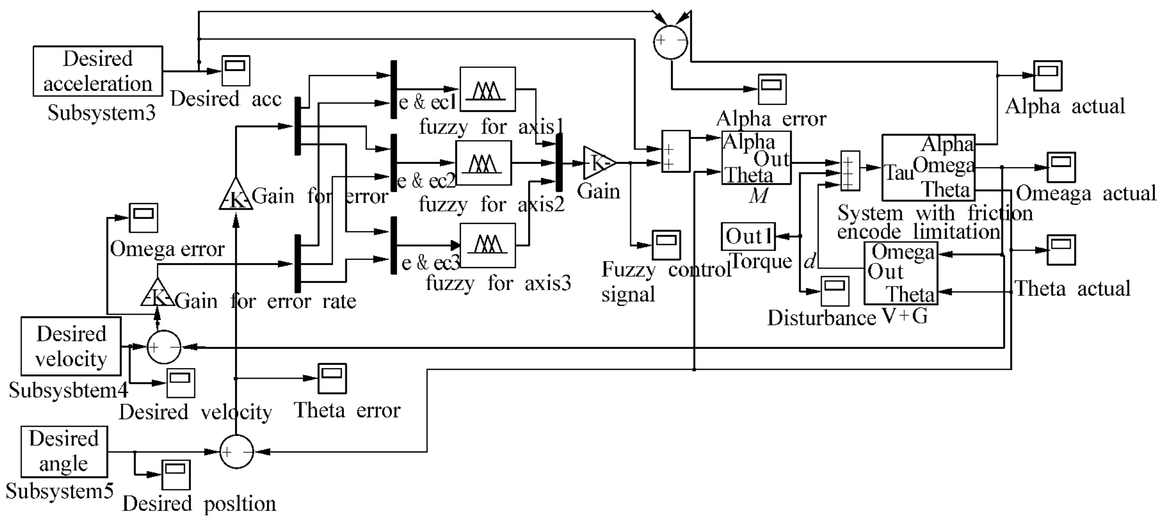

Fig. 5　Fuzzy logic controller with model-based portion

As there are many ways of implementing fuzzy logic in a control loop, it should be noted that this work only presents one of the possibilities. In this design, ehe derived simplified dynamics including friction forces are implemented in the Simulink/Matlab model as the ‘system’. The same set of equations, excluding those for friction forces, is also decomposed into a mass block, ‘M’ and others, ‘V + G’ without ‘F’. This arrangement has the friction forces only included in the system plant and not the model based portion. This arrangement reflects the un-modelled aspect of the system in the control loop to reflect real life modelling errors for the plant (named ‘system’ in Fig. 5). It will place larger burden on the controller to deal with such un-modelled dynamics. In addition, in the system block, the resolutions of encoders are set to be 0.001 53, 0.001 53, and 0.000 76 for axes 1, 2, and 3 respectively.

From an engineer's perspective, now the motion of a large piece of machinery can be controlled. The kinematics are accurately known but only simplified dynamics are obtained. There is still much that is unknown, including friction forces, disturbances (i. e. when gusty wind blows from time to time) and errors (resolution limitations) from encoders. With the known but incomplete mass and dynamics, it is possible to have a model-based port of control loop, which is shown in Fig. 5 as the M block and V + G block. With such a model-based portion, the load for fuzzy logic control can be lightened greatly as most of the dynamics would have been taken care of by the model-based portion.

Next, the input/output of the fuzzy logic portion needs to be considered. How much input/output is required? What are the weightings required to reflect the importance of the input signal? Is scaling necessary? If so, what are the appropriate scaling factors for input/output and should the same scaling factor be shared? Should all the input share the same fuzzy rules?

For the presented case, there are three axes to control, and the following decisions are made for the presented example. The same fuzzy rule set will be used by all three axes for motion control to simplify the case. Two inputs for each axis will be used for the fuzzy logic rules, the position error, and the velocity error, which are symbolised as e and e_c respectively in Fig. 5. Both input parameters are assumed to be in the range of [−3, 3] and can be changed if required. The output signal range is assumed to be [−4.5, 4.5] and the signals are divided into {NB, NM, NS, O, PS, PM, PB} where N represents negative, B represents big, M for medium, S for small, and P for positive. The logic rules are summarised in Table 2.

Table 2 Logic rule

e	e_c						
	NB	NM	NS	O	PS	PM	PB
NB	NB	NB	NM	NM	NS	NS	O
NM	NB	NM	NM	NS	NS	O	PS
NS	NM	NM	NS	NS	O	PS	PS
O	NM	NS	NS	O	PS	PS	PM
PS	NS	NS	O	PS	PS	PM	PM
PM	NS	O	PS	PS	PM	PM	PB
PB	O	PS	PS	PM	PM	PB	PB

One output for the control of each axis is produced as the fuzzy control signal. Two scaling factors are used as gain for the inputs with both having the numeric value of 50. One shared scaling factor for the output has a value of 0.000 1 for the presented case. Other combinations of these parameters may lead to better system performance than the presented combination. However, optimising the parameter combination is beyond the scope of this investigation.

4 Trajectory generation

Here, based upon the areas of stockpiles being reclaimed[8], it is assumed that the BWR is required to move from its initial position to the final position via three intermediate points to reclaim materials. The velocities passing all the points are assumed to be zero. The locations of those points observed from frame 0 in (x, y, z) format and required time are as follows.

1) Initial position: $p_i = (0, -11, 55)$ at time zero.

2) First intermediate position: $p_{\text{int}\,1} = (-35, -11, 32)$ at 200th second.

3) Second intermediate position: $p_{\text{int}\,2} = (-55, -11, 2)$ at 300th second.

4) Third intermediate position: $p_{\text{int}\,3} = (-38.5, -20, 50)$ at 500th second.

5) Final position: $p_f = (0, -11, 55)$ at 700th second.

First, inverse kinematics are applied to find the corresponding joint angles for those desired locations. Cubic polynomials are then used to generate the required trajectories (position, velocity, and acceleration) which pass through the required points[6]. The desired trajectories are shown in Fig. 6(a).

5 Simulation results and discussions

5.1 Desired vs. actual trajectories

The masses of the three links are assumed to be: m_1 = 2 500 kg; m_2 = 2 500 kg; and m_3 = 2 000 kg. These weights can be easily changed when more accurate values become available. Fig. 6(a) shows the desired BWR position trajectories of all three of the joints. Fig. 6(b) shows the actual position trajectories of all the joints. Solid lines are for joint 1 which is a prismatic joint, dot lines are for joint 2, and dash lines are for joint 3.

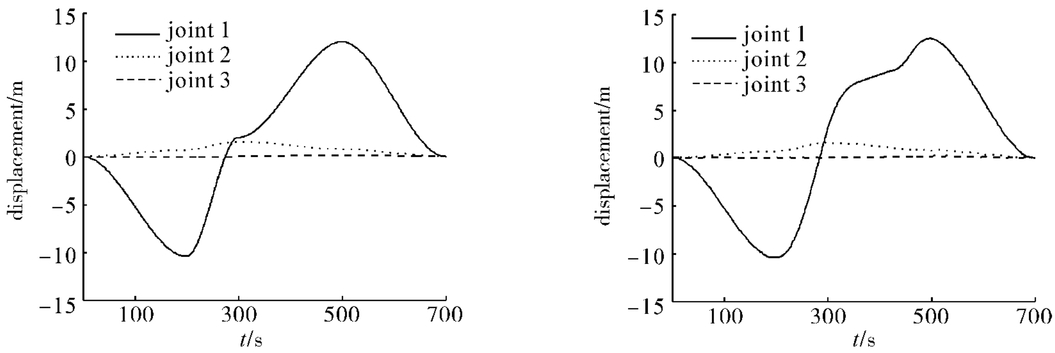

(a) Desired trajectory　　(b) Actual trajectory

Fig. 6　Position trajectories for the BWR in joint space

It an be seen from Fig. 6 that the BWR has successfully passed through all the points as required. The introduced encoder limitations, friction orces, and unexpected random disturbances applied at all the three joints have added an additional burden on the controller that seems to have been coped with reasonably well. However, there were some very minor ripples observed on the actual trajectories and as well as some deviations from the planned trajectory in some parts.

Fig. 7(a) shows the expected velocity trajectories of all three joints and Fig. 7(b) shows the actual velocity trajectories of all three joints. Fig. 8(a) shows the expected acceleration trajectories of all three joints and Fig. 8(b) shows the actual acceleration trajectories of all three joints.

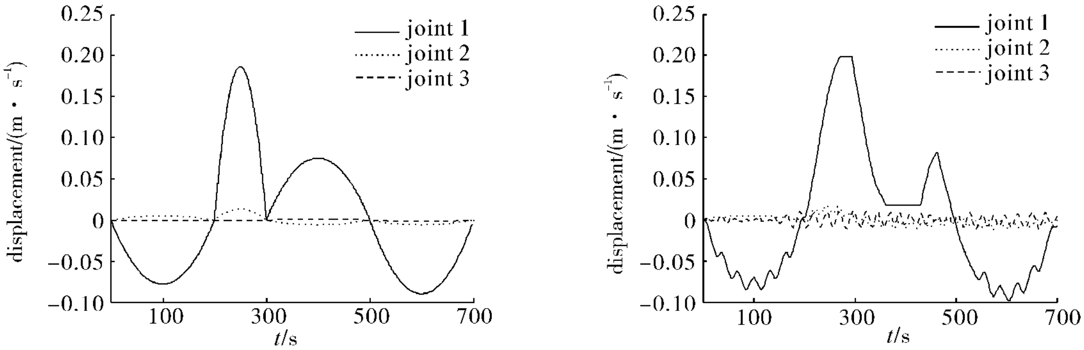

(a) Expected trajectory　　(b) Actual trajectory

Fig. 7　Velocity trajectories for the BWR in joint space

The actual velocity trajectory profiles shown in Fig. 7(b) basically follow the profiles of the desired trajectories shown in Fig. 7(a). However, the ripples shown in Fig. 7(b) seem to be related to the larger velocity switches as can be seen from Fig. 7(b). Similar effects can also be observed in Fig. 8 for the acceleration.

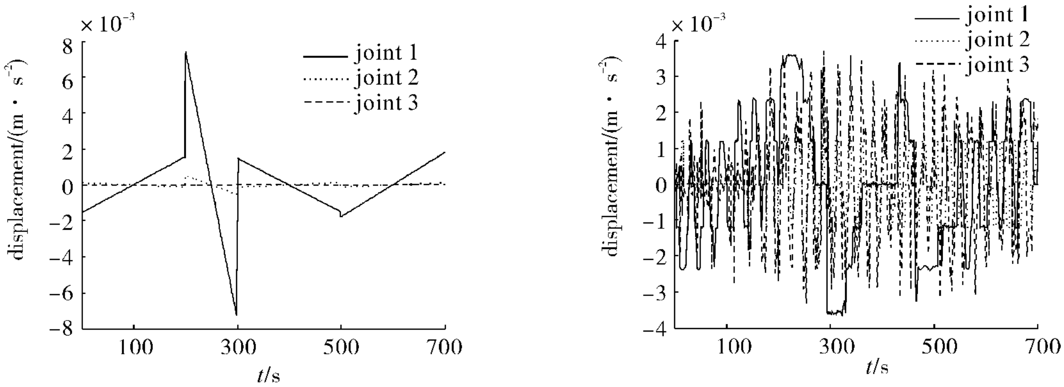

(a) Expected trajectory　　(b) Actual trajectory

Fig. 8　Acceleration trajectories for the BWR in joint space

5.2　Trajectory errors

Further investigation reveals that the velocity switching behaviours in Fig. 7 are caused mainly by the fuzzy logic control loop which has been applied. This is evident from Fig. 9 which shows the output from the fuzzy logic control signals that is used to control the motion of the system. Even though the averaged values come very close to the desired acceleration trajectories, the control signals produce something like digital switches for on (positive maximum or negative maximum) or off (zero).

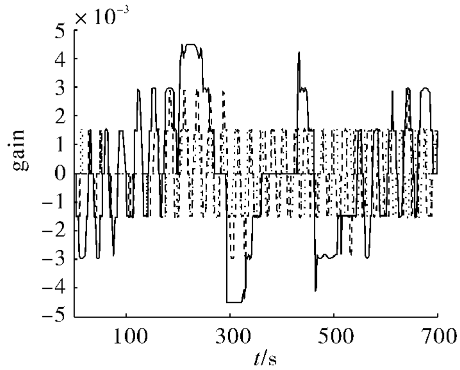

Fig. 9　Output control signals from fuzzy logic

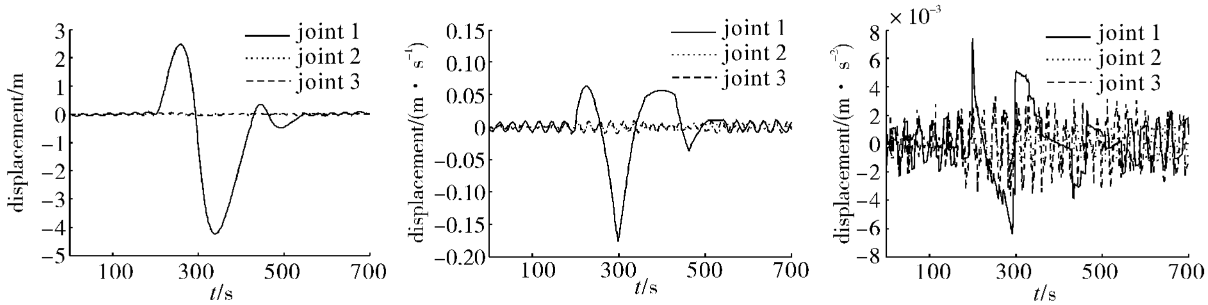

Fig. 10　Position, velocity, and acceleration errors (from left to right)

Fig. 10 shows the position, velocity, and acceleration errors. The maximum errors are -4 m at a time of around 340th of a second, $-0.17 \mathrm{m \cdot s^{-1}}$, and $0.007\,5\ \mathrm{m \cdot s^{-2}}$, respectively. Obviously, axis 1 has the most position errors deviating away from the desired trajectory which can be further improved as seen from the figure.

From an engineer's perspective, if the most important position trajectory-following target has been met, it might not be necessary to further investigate and improve the performance. Nevertheless, the parameters discussed in Section Ⅲ related to a fuzzy logic control loop and controller design are re-visited in the following section in order to improve system performance. It is understood that by changing the parameters and arrangement, differing system performances can be expected for better or worse.

5.3　Controller design modification and improved results

From Fig. 10, it is obvious that axis 1 has much larger errors in position, velocity, and acceleration trajectories, and therefore is focused upon here. From the errors, it does not appear appropriate to allow all three axes to share the same output gain, which has the value of 0.001, to multiply the control signals produced by fuzzy sets shared by the three axes according to the original controller design. Therefore, larger gains can be considered for use to enlarge the control signals and reduce the errors. Consequently, the shared gain needs to be divided into individual gains as the scale of error for each axis is different. The final individual gains selected for axis 1, 2 and 3 are 0.01, 0.04, and 0.06, respectively. They are all increased to reduce the errors, especially axis 1 which is 10 times higher than before. The modified controller design is shown in Fig. 11 below.

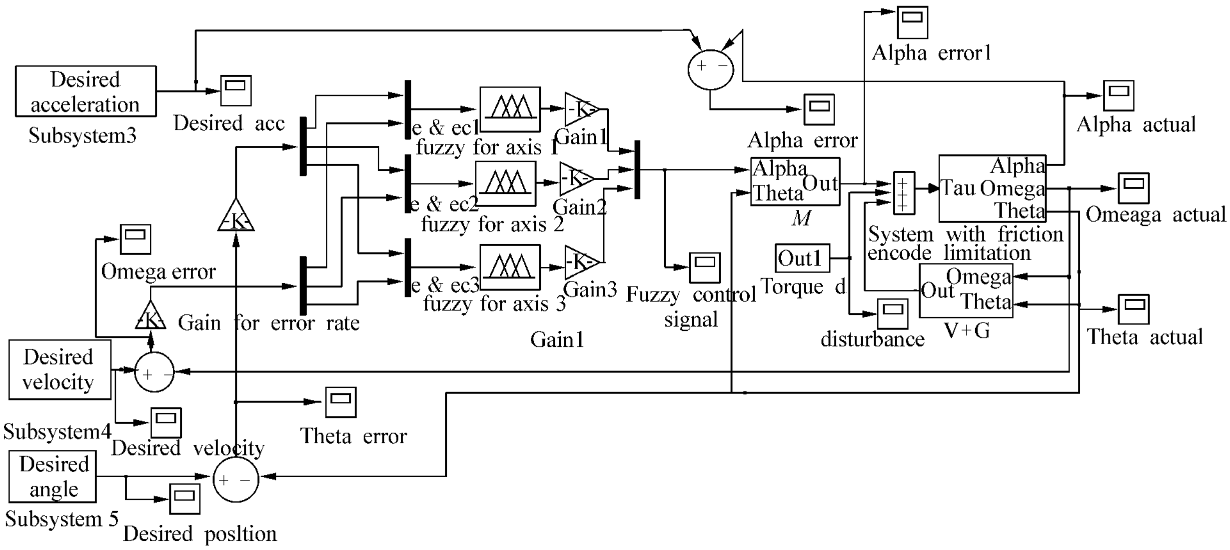

Fig. 11　Fuzzy logic controller with model-based portion and individual output gains

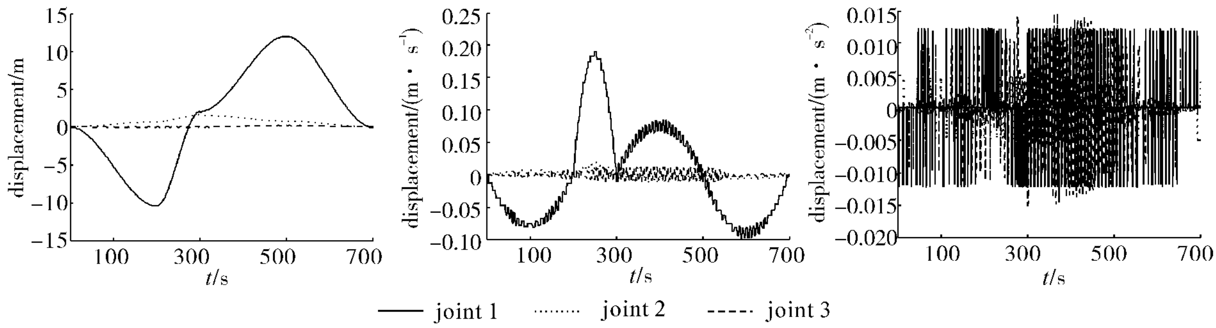

Fig. 12　Actual position, velocity, and acceleration trajectories (from left to right)

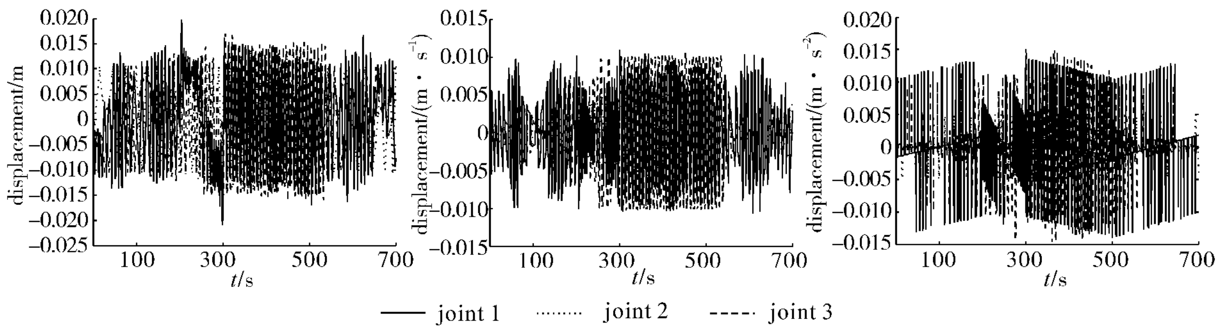

Fig. 13　Position, velocity, and acceleration errors (from left to right)

The resulting actual position, velocity, and acceleration trajectories are shown in Fig. 12 and the errors in Fig. 13. The maximum errors are now approximately 0.02 m at a time of around a 200th and 300th of a second, 0.01 m · s^{-1}, and 0.015 m · s^{-2} respectively, which is a significant improvement from the original controller design sharing output gains. Of course, there is no doubt that the system performance can be further improved, especially in the velocity and acceleration trajectories by changing factors such as the fuzzy rules, the gain values, and so on as mentioned in Section Ⅲ covering controller design. If the main target is changed from following the position trajectories to areas such as velocity trajectories, the fuzzy rules, and the gains, other aspects of the controller will need to be changed to produce satisfactory results. Nevertheless, this exercise demonstrates the presented model and simulation environment is capable of reflecting a real BWR and being used to develop appropriate control strategies for the physical control of a BWR.

6 Conclusion

This paper presents the implementation of fuzzy logic for the motion control of a large BWR to follow given trajectories in a simulated environment. The content covers the modelling of a typical BWR using Matlab/Simulink and includes not only the kinematics and simplified dynamics but also the friction forces from its joints, limitations of its encoder resolutions, and unexpected random disturbances to cover the un-modelled dynamics. Additionally, a hybrid controller, which consists of a fuzzy logic controller on top of a model based example, is developed and implemented. The paper provides engineers with an example of applying fuzzy logic together with a model based approach to properly control the motion of a large BWR to follow defined trajectories as well as possible ways to further improve the controller performance.

Acnowledgment

The authors would like to thank Australian Research Council and Industry Partner, Matrix Group Lty Ltd. for the financial and in-kind support through the ARC Linkage LP0989780 grant titled "The study and development of a 3-D real-time stockpile management system" and the support in part from Institute for Mineral and Energy Resources, University of Adelaide 2009-2010, as well as Faculty of Engineering, Computer and Mathematical Sciences strategic research funding, 2010.

References:

[1] LU Tienfu, XU Shihong. SPSim: a stockpile simulator for analyzing material quality distribution in mining[C]//International Conference on Mechatronics and Automation (ICMA 2010). Xi'an, China, 2010: 299-304.

[2] CHOI C, LEE K, SHIN K, et al. Inverse kinematics of a reclaimer: redundancy and solution[C]//IEEE International Conference on Systems, Man, and Cybernetics. Orlando, USA, 1997: 2883-2887.

[3] CHOI C, LEE K, SHIN K, et al. Automatic landing method of a reclaimer on the stockpile[J]. IEEE Transactions on Systems, Man, and Cybernetics—Part C: Applications and Reviews, 1999, 29(1): 308-314.

[4] HONG K S, CHOI C. Task-oriented approaches to the inverse kinematics problem for a reclaimer excavating and transporting raw material[J]. Advanced Robotics, 2000, 14(3): 185-204.

[5] LU Tienfu. Bucket wheel reclaimer modelling as a robotic arm[C]//IEEE International Conference on Robotics and Biomimetics. Guilin, China, 2009: 263-268.

[6] LU Tienfu. Preparation for turning a bucket wheel reclaimer into a robotic arm[C]//IEEE International Conference on Robotics and Biomimetics. Bangkok, Thailand, 2008: 1710-1715.

[7] LU Tienfu, LIN G C. Intelligent systems techniques and their application in manufacturing systems[M]//LEONDES C T. Expert systems: the technology of knowledge management and decision making for the 21st century. San Diego, USA: Academic Press, 2002: 381-410.

[8] LU Tienfu, MYO M T R. Optimization of reclaiming voxels for quality grade target with reclaimer minimum movement [C]//The Eleventh International Conference on Control, Automation, Robotics and Vision (ICARCV 2010). Singapore, 2010: 1350-1410.

About the author:

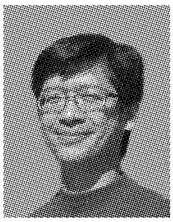

LU Tienfu received his Bachelor of Science and Master of Science in Mechanical Engineering from National Cheng Kung University, Taiwan in 1988 and 1990 respectively. He received his PhD in Manufacturing and Mechanical Engineering from the University of South Australia in 1997. He was a postdoctoral researcher at the University of South Australia between 1997 and 2000. Since 2001, he has been with the School of Mechanical Engineering, University of Adelaide and is currently a senior lecturer. He is the leader of the robotics research lab at the University of Adelaide and his current research interests include intelligent mobile robotics (modelling, trajectory planning, localisation, and navigation), underwater robotics (modelling, localisation, and navigation), insect robotics (chemical plume source localisation), mechatronic technologies in mining, and micro-motion robotic systems (pzt actuator modelling and control, and micro-motion stages). He is a member of the IEEE and currently an associate Editor of the Australian Journal of Mechanical Engineering (AJME), Engineers Australia, and a member of the International Journal of Intelligent Mechatronics and Robotics (IJIMR) Editorial Board. He has so far published one Australian provisional patent, three book chapters, 26 journal papers and more than 80 conference papers.